Optical properties of heavily doped GaN/(Al,Ga)N multiple quantum wells grown on 6*H*-SiC(0001) by reactive molecular-beam epitaxy

A. Thamm, O. Brandt, J. Ringling, A. Trampert, and K. H. Ploog
Paul-Drude-Institut für Festkörperelektronik, Hausvogteiplatz 5–7, D-10117 Berlin, Germany

O. Mayrock, H.-J. Wünsche, and F. Henneberger
Humboldt-Universität zu Berlin, Invalidenstrasse 110, D-10115 Berlin, Germany
(Received 21 October 1999; revised manuscript received 10 March 2000)

We study, both experimentally and theoretically, the influence of polarization-induced electric fields on the optical properties of heavily doped ($7\times10^{18}\,\mathrm{cm}^{-3}$) GaN/(Al,Ga)N multiple-quantum-well structures. To investigate the impact of the strain state on the transition energy, these heterostructures are deposited on either a GaN or an (Al,Ga)N relaxed buffer layer. Furthermore, we show that the recombination dynamics in these heavily doped multiple quantum wells is still controlled by residual electric fields, contrary to the common assumption that flatband conditions are established at this doping level.

Recently, strong polarization-induced electrostatic fields have been found to lead to unusual optical and electrical properties of GaN/(Al,Ga)N multiple quantum wells (MQW's).[1,2] In fact, even the optical properties of unstrained GaN quantum wells (QW's) can only be explained by strong electric fields in the wells, which can be attributed to the interplay of polarization-induced electric fields in the well and barrier layers due to the alignment of the Fermi level.[3] The electric field within the QW's leads to a quantum-confined Stark effect (QCSE) of the QW emission, which thus can fall well below the bulk band-gap energy. Due to the spatial separation of the electron and hole wave functions, the oscillator strength of these transitions may become many orders of magnitude smaller than under field-free conditions. This fact has important consequences for the optical properties of nitride-based light-emitting diodes and lasers.

Piezopolarization is generated in noncentrosymmetric crystals via external stress induced, e.g., by coherent growth of materials with dissimilar lattice constants. The sign of the piezopolarization depends on both the polarity of the crystal and on the sign of the strain, i.e., whether it is compressive or tensile. *Spontaneous polarization* is created by the singular polar axis of the wurtzite structure. The sign of the spontaneous polarization only depends on the polarity of the layer. For group-III nitrides, both piezopolarization and spontaneous polarization constants have been calculated theoretically.[4] At the interface of two materials with different net polarizations, the surplus of polarization charges creates fields up to 5 MV/cm, as long as the potential drop across the *c* axis of the layer is lower than the band gap.[5] For the GaN/(Al,Ga)N material system, the individual contributions of piezopolarization and spontaneous polarization to the total field are roughly equal.

In this paper, we investigate the influence of the strain state on the polarization fields and their screening by heavy doping in GaN/(Al,Ga)N MQW's. Two sets of heavily doped ($7\times10^{18}\,\mathrm{cm}^{-3}$) GaN/$Al_{0.15}Ga_{0.85}N$ MQW's (15 periods) with well thicknesses ranging from 1.5 to 7.5 nm are grown under the same conditions on 1-μm-thick GaN and $Al_{0.15}Ga_{0.85}N$ buffer layers, respectively. The total thickness of the MQW's is below the critical thickness and hence either the $Al_{0.15}Ga_{0.85}N$ barrier layers or the GaN QW's are strained. We study the optical properties of these structures by both stationary and time-resolved photoluminescence and compare our findings with the results of self-consistent Schrödinger-Poisson calculations. Commonly it is assumed that high-carrier densities screen polarization fields effectively, so that flatband conditions are established.[6] We demonstrate that this assumption is too naive. First of all, with increasing doping level we may only approach the band profile of a very heavily doped heterostructure, but not that of an undoped and field-free structure which is commonly taken to represent flatband conditions. Electrons thus persist to be localized up to very high doping levels at the potential spikes created by electron accumulation and depletion zones, respectively, which are inevitably linked to heavy doping. Second, the transition energy for thick wells may approach (but never reach) the (not-renormalized) bulk gap energy for intermediate to high doping levels due to the interplay of screening and band-gap renormalization. Finally, we show that the strain state of the QW's—unstrained for the GaN buffer, and compressively strained for the (Al,Ga)N buffer—alone has little impact on the electric fields.

Growth is carried out in a custom-designed two-chamber molecular-beam-epitaxy (MBE) system equipped with conventional Ga and Al effusion cells and an unheated NH_3 gas injector. The as-received 6*H*-SiC(0001) substrates from Cree Research (on-axis Si face) are etched *ex situ* by H_2 at 1600 °C for 20 min to remove the polishing scratches and the damage layer present on these substrates. Details of the growth conditions can be found in Ref. 7. For doping, we deactivate the NH_3 filter, resulting in background electron concentrations of $7\times10^{18}\,\mathrm{cm}^{-3}$ [as determined by Hall measurements of GaN reference layers grown on semi-isolating 4*H*-SiC(0001)] due to the incorporation of O from residual moisture[8] contained in NH_3. In contrast to Si doping, this procedure has the advantage of being highly reproducible, since O is incorporated at its solubility limit. After growth, the MQW structures are characterized by several techniques.

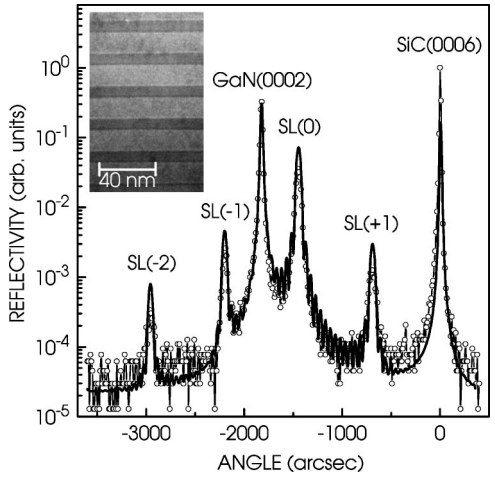

FIG. 1. ω-2Θ scan of a 15-period (7.5 nm) GaN/(14.6 nm) $Al_{0.15}Ga_{0.85}N$ MQW structure (open symbols). Note the sharp superlattice reflections and the excellent fit by dynamical diffraction theory (solid line). The cross-sectional TEM micrograph (inset) of a part of the multilayer structure reveals microscopically abrupt heterointerfaces (Ref. 9).

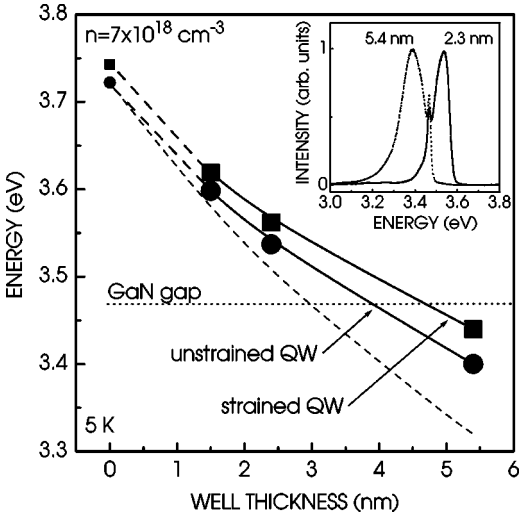

FIG. 2. Thickness-dependent shift of the PL maximum for unstrained (circles) and compressively strained (squares) wells compared to undoped QW's (dashed line). The solid lines are a guide to the eye. The emission energies of the $Al_{0.15}Ga_{0.85}N$ barriers are plotted at zero well thickness. The inset shows the spectra of a thin (2.3 nm) and a thick (5.4 nm) unstrained GaN QW.

X-ray diffractometry (XRD) ω-2Θ scans recorded in triple-crystal configuration are used for determining the thicknesses of the individual layers as well as the Al composition. The latter is kept constant for all structures and found by the x-ray measurements to be 0.15 ± 0.01. Transmission electron microscopy (TEM) is carried out with a JEOL 4000EX operating at 400 kV. The optical properties at 5 K are studied by continuous-wave (cw-PL) and time-resolved (ps-PL) photoluminescence spectroscopy, employing the 325-nm line of a 50-mW He-Cd laser and a frequency-tripled Ti:sapphire laser with a pulse width of about 400 fs and a repetition rate of 76 MHz for excitation, respectively.

Figure 1 shows an ω-2Θ scan of one of the $GaN/Al_{0.15}Ga_{0.85}N$ MQW's on a GaN buffer layer. Intense and sharp superlattice peaks SL($\pm n$) up to second order are observed, as well as Pendellösung fringes in the vicinity of the GaN(0002) reflection, indicating a high periodicity and abrupt heterointerfaces. Indeed, this presumption is confirmed by TEM (see the inset of Fig. 1). Fits to the experimental x-ray data based on dynamic diffraction theory (solid line) allow us to accurately determine the structural parameters, namely the Al content (0.15 ± 0.005) and the well (7.5 ± 0.15 nm) and barrier (14.6 ± 0.15 nm) thicknesses. The agreement between simulation and experiment shows the excellent structural quality of the sample.

The transition energies of unstrained and compressively strained GaN QW's with different well thickness are compiled in Fig. 2. The inset shows the PL spectra of two MQW's grown on a GaN buffer (due to stress-induced cracks, PL from the GaN buffer is seen at 3.467 eV). As expected, the emission of the thin wells (1.5 and 2.3 nm) is strongly blueshifted with respect to the bulk GaN band gap due to the quantum confinement. Thicker wells (5.4 nm) do emit slightly below the bulk GaN band gap, suggesting that the internal fields are not screened completely despite the high doping level. The residual fields amount to about half of the theoretical value of 1.58 MV/cm for zero doping density (dashed line). A rigid shift of 30 ± 10 meV is observed between unstrained and compressively strained QW's, which is in agreement with the theoretical value for the increase of the GaN gap under a compressive biaxial strain of $+0.4\%$.[10] In fact, the difference in polarization field strength between QW's under this strain state and unstrained QW's is predicted to be only about 3%.[5]

Figure 3 shows the PL transients for unstrained (a) and compressively strained GaN QW's (b). For the same well thicknesses, the decay times are comparable for both strain states. While the decay times for the thin QW's are within expectation (300–400 ps), the long decay times (2–4 ns) for the thick QW's come as a surprise (the decay times of the thickest QW's are too long to be measured with our setup, which is why they are excluded from our analysis). In fact, a complete screening of the fields should result in decay times basically independent of the well width. Even incomplete screening is intuitively expected to result in a drastic increase of electron-hole overlap, and thus in an equally drastic reduction of carrier lifetime. Note that these experiments are done within the small-signal regime ($<10^{17}\,\mathrm{cm}^{-3}$), so that a

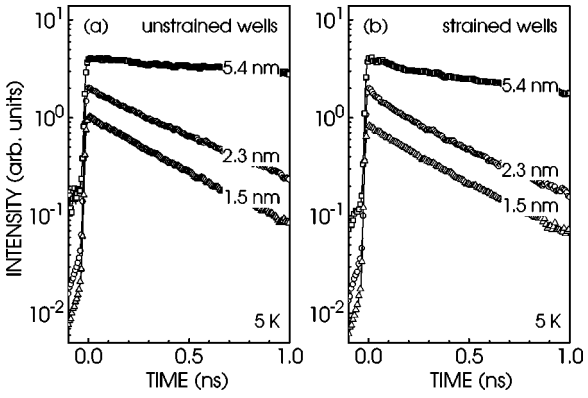

FIG. 3. PL transients of $GaN/Al_{0.15}Ga_{0.85}N$ MQW's with various well widths for unstrained (a) and compressively strained (b) wells.

TABLE I. Parameters used for the self-consistent calculations of $GaN/Al_{0.15}Ga_{0.85}N$ MQW's

Parameter	GaN	$Al_{0.15}Ga_{0.85}N$
E_g (eV)	3.5	3.74
n (cm^{-3})	7×10^{18}	7×10^{18}
e_{31} (C/m^2)	-0.49[a]	-0.5065[a]
e_{33} (C/m^2)	0.73[a]	0.8395[a]
P_{Sp} (C/m^2)	-0.029[a]	-0.0368[a]
C_{13} (GPa)	103[b]	104[b]
C_{33} (GPa)	405[b]	400[b]
ϵ_r	9.77	9.58
m_e/m_0	0.2	0.22
m_h/m_0	1.0	1.0
$\Delta E_C/\Delta E_V$		70/30

[a]Bernardini *et al.* (Ref. 5).
[b]Wright (Ref. 11).

dynamic screening of the internal electric fields is not to be expected. In fact, the PL lines do not exhibit spectral diffusion, nor does their temporal behavior depend on excitation density.

For a more quantitative treatment concerning the magnitude of the residual fields, we perform self-consistent Schrödinger-Poisson calculations using the piezoelectric and spontaneous polarization constants from Ref. 5. All parameters used for the simulations are listed in Table I. These calculations include the correction of the transition energy by the exciton binding energy[12] in the case of electron densities below the Mott transition, and band-gap renormalization due to many-body effects in high-density electron gases above the Mott transition. The latter effect is estimated by first-order perturbation theory of the electron-electron exchange energy. Concerning the comparison of experiment and simulation, the following consideration is worth noticing. Regardless of the position of the Fermi level at the surface, it is obvious that the MQW experiences a superimposed depletion field, influencing those QW's being in the close vicinity of the surface. The altered band-edge alignment in these QW's gives rise to different transition energies and thus contributes to a broadening of the total PL line. In our calculation, we neglect this phenomenon, and give instead the transition energy (and overlap) for the third QW which is already

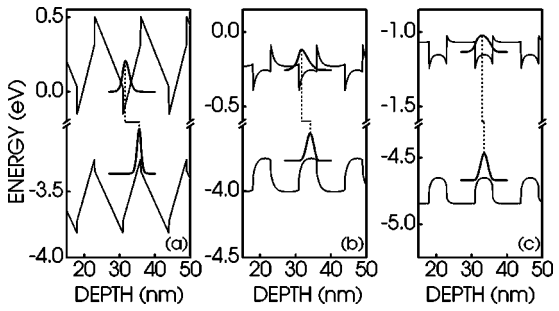

FIG. 4. Band profiles of a $[(5\text{ nm})\,GaN/(8\text{ nm})\,Al_{0.15}Ga_{0.85}N]_{15}$ MQW for carrier concentrations of (a) $1\times10^{15}\,cm^{-3}$, (b) $1\times10^{20}\,cm^{-3}$, and (c) $1\times10^{21}\,cm^{-3}$. Note the residual potential spike for a concentration of $1\times10^{20}\,cm^{-3}$, localizing the electron wave function.

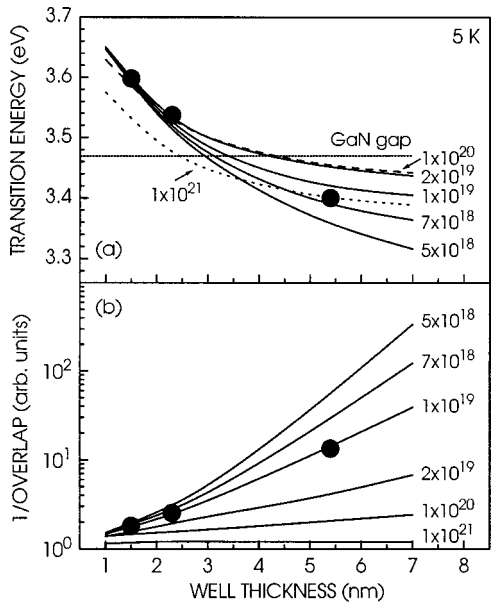

FIG. 5. Well thickness and doping density dependence of (a) transition energy and (b) reciprocal electron-hole overlap for unstrained QW's. Note the agreement with the experiment (circles) for the measured carrier concentration of 7×10^{18} cm^{-3}. The measured carrier lifetimes (b) are normalized by a constant factor assuming $\tau_{n\tau}\gg\tau_\tau$ for the well thickness of1.5 nm.

outside of the depletion width for the doping level under consideration. Note, however, that undoped MQW's may experience an inhomogeneous field distribution to a depth of several 100 nm.

The self-consistently calculated band-edge profiles and subband wave functions of unstrained 5-nm GaN QW's for various doping densities are plotted in Fig. 4. Evidently, the electron wave function persists to be localized at the upper GaN/(Al,Ga)N interface up to electron concentrations of about $10^{20}\,cm^{-3}$, resulting in a strong reduction of the

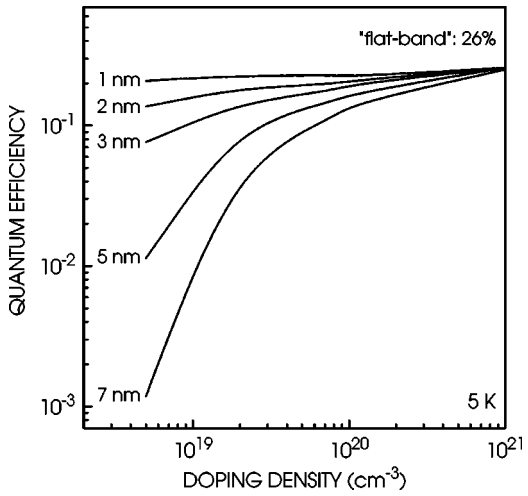

FIG. 6. Doping and thickness dependence of the internal quantum efficiency for unstrained QW's. The ''flatband'' quantum efficiency was set arbitrarily to 26%. The nonradiative contribution is assumed to be independent of well thickness and doping. Note the strong dependence of the quantum efficiency on well thickness even for doping levels in the regime of $10^{19}\,cm^{-3}$.

electron-hole overlap and thus in an increase of the radiative lifetime. Only for electron concentrations in the regime of $10^{21}\,\mathrm{cm}^{-3}$ does the band profile become almost symmetrical and the electron wave function shifts into the center of the well, thus maximizing the overlap. Still, even at the highest doping levels we never reach flatband conditions, i.e., the band profile of an undoped and field-free structure.

Figure 5 displays a comparison of our experimental data with the calculated transition energies and reciprocal electron-hole overlap as a functions of the well width for various electron concentrations (only the case of unstrained wells is shown). As seen in Fig. 5(a), the transition energy initially increases with doping due to screening, but then decreases again due to band-gap renormalization. At intermediate doping levels, the transition energy for thick wells is coincidentally quite close to the unrenormalized bulk band gap. While this finding may suggest an essentially complete screening of the internal fields,[1,6] the corresponding PL decay times [Fig. 5(b)] still increase with well thickness at these carrier densities. This fact demonstrates that the electron-hole overlap is reduced up to very high doping levels, as indicated in Fig. 4.

This reduction in electron-hole overlap will of course not matter in ideal structures with an internal quantum efficiency of unity.[13] However, the situation is different provided that a nonvanishing nonradiative recombination channel exists, which can safely be assumed for GaN-based structures. Nonradiative recombination will reduce the internal quantum efficiency $\eta=(1+\tau_r/\tau_{\mathrm{nr}})^{-1}$ (where τ_r and τ_{nr} are the radiative and nonradiative lifetime, respectively) roughly in proportion to the radiative lifetime. In fact, in our experiments the ratio between the PL intensity at 300 and 4 K sharply decreased with increasing well thickness. This decrease of quantum efficiency (Fig. 6) results, for example, in a decreasing luminous efficiency P of light-emitting diodes ($P\sim\eta$) and in an increase of the threshold current density[13] j_{th} in injection lasers ($j_{\mathrm{th}}\sim\eta^{-1}$).

In summary, we have shown that the strain state of the GaN well in MQW's alters the piezoelectric fields only slightly. Furthermore, while the transition energy in heavily doped structures may suggest that complete screening is achieved, the recombination dynamics is still severely affected up to carrier concentrations of $10^{20}\,\mathrm{cm}^{-3}$. Carriers are localized at the potential spikes created by electron accumulation and depletion zones, respectively, which are inevitably linked to heavy doping. The reduced electron-hole overlap leads to a significant reduction of the internal quantum efficiency and therefore emitter performance.

We acknowledge financial support by the Volkswagen-Stiftung. The authors thank M. Reiche for x-ray measurements, H. von Kiedrowski for SiC etching, H.-P. Schönherr for assistance in MBE technology, and G. Apostolopoulos for invaluable help with the XRD simulation.

[1] A. Hangleiter, J. S. Im, H. Kollmer, J. Off, and F. Scholz, MRS Internet J. Nitride Semicond. Res. **3**, 15 (1998).
[2] H. S. Kim, J. Y. Lin, H. X. Jiang, W. W. Chow, A. Botchkarev, and H. Morkoç, MRS Internet J. Nitride Semicond. Res. **4**(S1), G3.3 (1999).
[3] R. Langer, J. Simon, V. Ortiz, N. T. Pelekanos, A. Barski, R. André, and M. Godlewski, Appl. Phys. Lett. **74**, 3837 (1999).
[4] F. Bernardini, V. Fiorentini, and D. Vanderbilt, Phys. Rev. B **56**, R10 024 (1997).
[5] F. Bernardini and V. Fiorentini, Phys. Rev. B **57**, R9427 (1998).
[6] F. Della Sala, A. Di Carlo, F. Bernardini, V. Fiorentini, R. Scholz, and J.-M. Jancu, Appl. Phys. Lett. **74**, 2002 (1999).
[7] A. Thamm, O. Brandt, Y. Takemura, A. Trampert, and K. H. Ploog, Appl. Phys. Lett. **75**, 944 (1999).
[8] W. Kim, A. E. Botchkarev, A. Salvador, G. Popovici, H. Tang, and H. Morkoç, J. Appl. Phys. **82**, 219 (1997).
[9] As a result of the improved substrate preparation, the dislocation density estimated from plan-view micrographs (not shown here) is below $10^9\,\mathrm{cm}^{-2}$. This result is confirmed by the linewidths of x-ray rocking curves which are found to be 200 and 750 arcsec for symmetric and asymmetric reflections, respectively.
[10] P. Waltereit, O. Brandt, A. Trampert, M. Ramsteiner, M. Reiche, M. Qi, and K. H. Ploog, Appl. Phys. Lett. **74**, 3660 (1999).
[11] A. F. Wright, J. Appl. Phys. **82**, 2839 (1997).
[12] R. P. Leavitt and J. W. Little, Phys. Rev. B **42**, 11 774 (1990); P. Peyla *et al.*, *ibid.* **52**, 12 026 (1995).
[13] S.-H. Park, S.-L. Chuang, and D. Ahn, Appl. Phys. Lett. **75**, 1354 (1999).